Journal of Applied Analysis and Computation
Volume 15, Number 1, February 2025, 226–244
Website:http://www.jaac-online.com
DOI:10.11948/20240078

ENHANCING SOLUTIONS FOR NON-LINEAR ORDINARY DIFFERENTIAL EQUATIONS VIA COMBINED LAPLACE TRANSFORM AND REPRODUCING KERNEL METHOD

Ali Akgül[1,2] and Nourhane Attia[3,†]

Abstract Ordinary differential equations (ODEs) describe diverse phenomena in engineering and physics, such as electrical networks, oscillating systems, satellite orbits, and chemical reactions. Solving these equations, particularly the non-linear ones, is often challenging due to their complexity. This study aims to innovate by integrating the Laplace transform with the reproducing kernel Hilbert space method (RKHSM), introducing an enhanced approach that surpasses classical RKHSM. The combined Laplace-RKHSM method simplifies the original non-linear ODEs, allowing for the construction of novel numerical solutions. These solutions are systematically obtained in series form, providing both analytic and approximate results. The effectiveness and efficacy of the Laplace-RKHSM are demonstrated through three applications, each showcasing the method's superior performance in terms of accuracy and computational efficiency. This new approach not only enhances the existing RKHSM but also broadens its applicability to a wider range of non-linear problems in physics and engineering.

Keywords Reproducing kernel method, Laplace transformation, non-linear ODEs, numerical approximation.

MSC(2010) 46E22, 34A08.

1. Introduction

The ordinary differential equations are of great importance because of their ability to describe numerous phenomena in physics such as electrical networks, oscillating and vibrating systems, satellite orbits, chemical reactions, and so on [5,6,22,28,30]. Finding the ODEs' solutions is the key to understanding nature, but it is hard and sometimes impossible to get the exact solutions of most real-life ODEs, especially the non-linear ones. And for such a case, one resorts to numerical methods. That's why developing numerical methods to solve complex non-linear problems has become a

†The corresponding author.
[1]Siirt University, Art and Science Faculty, Department of Mathematics, 56100 Siirt, Turkey
[2]Department of Computer Science and Mathematics, Lebanese American University, Beirut, Lebanon
[3]National High School for Marine Sciences and Coastal (ENSSMAL), Dely Ibrahim University Campus, Bois des Cars, B.P. 19, 16320, Algiers, Algeria
Email: ali.akgul@lau.edu.lb(A. Akgül),
nourhane.attia@enssmal.edu.dz(N. Attia)

crucial task for researchers.

The RKHSM is a widely used numerical method for solving non-linear ODEs (NODEs). This method that was proposed in 1908 [31] is an effective numerical method for complex nonlinear problems without discretization. Many researchers applied it to solve several types of equations [1–4,9–13,15–21,23–27,29]. Its principal advantages are the feature that is it is easy to be applied, especially because it is meshfree, and its capability to deal with diverse complex differential equations.

The question behind this research is: "What will this efficient method be if we combine it with an operator that makes the differential equations simpler to handle?". This question pushed us to suggest a new numerical method for the NODEs. This research aims to provide a new convenient method using the reproducing kernel (RK) theory and the Laplace transform operator for obtaining the non-linear ODEs' solutions.

In this paper and for the first time, the Laplace-RKHSM (L-RKHSM) is used for constructing numerical solutions for the non-linear ODEs. Its general methodology is: First, we need to obtain a simpler non-linear ODE than the original one using the Laplace transform. Then, we apply the RKHSM. One of the powerful advantages of this new method is we can obtain better results than the classical RKHSM with a minute number of iterations.

The next section shows some basic definitions and theorems concerning RK theory and Laplace transform operator. The description of the L-RKHSM and its application to the proposed problem are presented in the third section. The L-RKHSM's effectiveness and the solutions' accuracy are validated through three applications in the fourth section. Finally, the conclusion is given.

2. Preliminaries

To use the Laplace-RKHSM, we should present some definitions and theorems from RK theory and calculus.

Definition 2.1. The Laplace transform of a function $f(\varsigma)$, $\varsigma \geq 0$ is the integral [7]:

$$\mathcal{L}[f(\varsigma)] = F(s) = \int_0^\infty \exp(-s\varsigma) f(\varsigma) d\varsigma.$$

Definition 2.2. A function $N : ß \times ß \to \mathbb{C}$ is called a reproducing kernel of H if [14]

1. $N(\cdot, \varsigma) \in H$, $\forall \varsigma \in ß$.
2. (Reproducing property.) $\langle f, N(\cdot, \varsigma)\rangle = f(\varsigma)$, $\forall f \in H$ and $\forall \varsigma \in ß$.

Where H is a Hilbert space over $ß \neq \varnothing$.

Definition 2.3. A function space $W_2^2[0,T]$ is [14]

$$\begin{aligned} W_2^2[0,T] =& \{f(\varsigma) | \text{ The functions } f \text{ and } f' \text{ are absolutely continuous in } [0,T], \\ & f'' \in L^2[0,T], \text{and } f(0) = 0\}, \end{aligned}$$

with the inner product:

$$\langle f, g\rangle_{W_2^2} = \sum_{j=0}^{1} f^{(j)}(0) g^{(j)}(0) + \int_0^T f''(\varsigma) g''(\varsigma) d\varsigma,$$

and norm:

$$\|f\|_{W_2^2} = \sqrt{\langle f, f\rangle_{W_2^2}},$$

for all $f, g \in W_2^2[0,T]$.

Theorem 2.1. *The reproducing kernel function $S_\tau(\varsigma)$ of $W_2^2[0,T]$, given by* [8]

$$S_\tau(\varsigma) = \begin{cases} \varsigma\tau + \frac{1}{2}\varsigma^2\tau - \frac{1}{6}\varsigma^3 \ , \ \varsigma \leq \tau, \\ \tau\varsigma + \frac{1}{2}\tau^2\varsigma - \frac{1}{6}\tau^3 \ , \ \varsigma > \tau. \end{cases}$$

For the proof of this theorem, see [8].

Definition 2.4. A function space $W_2^1[0,T]$ is [14]

$$W_2^1[0,T] = \{f(\varsigma) | \text{ The function } f' \text{ is absolutely continuous in } [0,T], f' \in L^2[0,T]\},$$

with the inner product:

$$\langle f, g\rangle_{W_2^1} = f(0)g(0) + \int_0^T f'(\varsigma)g'(\varsigma)d\varsigma,$$

and norm:

$$\|f\|_{W_2^1} = \sqrt{\langle f, f\rangle_{W_2^1}},$$

for all $f, g \in W_2^1[0,T]$.

Theorem 2.2. *The reproducing kernel function $R_\tau(\varsigma)$ of $W_2^1[0,T]$, given by* [8]

$$R_\tau(\varsigma) = \begin{cases} 1 + \varsigma \ , \varsigma \leq \tau, \\ 1 + \tau \ , \varsigma > \tau. \end{cases}$$

For the proof of this theorem, see [8].

3. Solution methodology

We now consider the 1st-order non-linear ordinary differential equation,

$$\begin{cases} f'(\varsigma) = H(\varsigma, f(\varsigma)), & \varsigma \in [0,T], \ T \in \mathbb{R}^*, \\ f(0) = \lambda. \end{cases} \tag{3.1}$$

Where f is the unknown, H is a function of ς and $f(\varsigma)$, and λ is a constant.

The idea of this new method is to take the Laplace transform of both sides of (3.1) as a first step. Then, we apply the classical RKHSM. One of the powerful advantages of the Laplace transform operator is that it makes the ordinary differential equation simpler to be solved and that's why we propose in this paper to combine the Laplace transform operator with the RKHSM. So, let us apply the following steps:

The first step is to homogenize the initial condition $f(0) = \lambda$ by suitable transformation. To do so, the change of variable has the form:

$$g(\varsigma) = f(\varsigma) - \lambda. \tag{3.2}$$

Using this transformation, (3.1) becomes

$$\begin{cases} g'(\varsigma) = \bar{H}(\varsigma, g(\varsigma)), & \varsigma \in [0, T],\ T \in \mathbb{R}^*, \\ g(0) = 0, \end{cases} \tag{3.3}$$

where $\bar{H}$ is a function of ς and $g(\varsigma)$. Now, applying the Laplace transform to (3.3):

$$\mathcal{L}\left[g'(\varsigma)\right] = \mathcal{L}\left[\bar{H}(\varsigma, g(\varsigma))\right].$$

So, by s-shift,

$$s\mathcal{L}\left[g(\varsigma)\right] - g(0) = \mathcal{L}\left[\bar{H}(\varsigma, g(\varsigma))\right].$$

Some algebra gives

$$\mathcal{L}\left[g(\varsigma)\right] = \frac{1}{s}\,\mathcal{L}\left[\bar{H}(\varsigma, g(\varsigma))\right].$$

Then, taking the Laplace transform of this latter, we reach

$$g(\varsigma) = \mathcal{L}^{-1}\left[\frac{1}{s}\,\mathcal{L}\left[\bar{H}(\varsigma, g(\varsigma))\right]\right].$$

Then, (3.1) becomes

$$\begin{cases} g(\varsigma) = \Lambda(\varsigma, g(\varsigma)),\ \varsigma \in [0, T], \\ g(0) = 0, \end{cases}$$

where $\Lambda(\varsigma, g(\varsigma)) = \mathcal{L}^{-1}\left[\frac{1}{s}\,\mathcal{L}\left[\bar{H}(\varsigma, g(\varsigma))\right]\right]$.

The last step is to apply the classical RKHSM and we start with introducing a linear operator $\mathfrak{O} : W_2^2[0, T] \to W_2^1[0, T]$ defined by

$$\mathfrak{O}g(\varsigma) = g(\varsigma).$$

So, using the linear operator we introduced, we get

$$\begin{cases} \mathfrak{O}g(\varsigma) = \Lambda(\varsigma, g(\varsigma)),\ \varsigma \in [0, T], \\ g(0) = 0, \end{cases} \tag{3.4}$$

where $\Lambda(\varsigma, g(\varsigma)) = \mathcal{L}^{-1}\left[\frac{1}{s}\,\mathcal{L}\left[\bar{H}(\varsigma, g(\varsigma))\right]\right]$.

One of the essential steps for applying the RKHSM is the construction of an orthogonal function system of $W_2^2[0, T]$. To do so, let

$$\psi_{\mathfrak{i}}(\varsigma) = \mathfrak{O}^*\kappa_{\mathfrak{i}}(\varsigma),$$

where

- $\kappa_{\mathfrak{i}}(\varsigma) = R_{\varsigma_{\mathfrak{i}}}(\varsigma)$, in which $R_{\varsigma_{\mathfrak{i}}}(\varsigma)$ represents the RK function of $W_2^1[0, T]$.
- The set $\{\varsigma_{\mathfrak{i}}\}_{\mathfrak{i}=1}^{\infty}$ is dense in $[0, T]$.

- $\mathfrak{O}^*$ denotes the adjoint of $\mathfrak{O}$.

Based on Gram-Schmidt's process, we find $\{\bar{\psi}_{\mathfrak{i}}\}_{\mathfrak{i}=1}^{\infty}$ as:

$$\bar{\psi}_{\mathfrak{i}}(\varsigma) = \sum_{k=1}^{\mathfrak{i}} \varpi_{\mathfrak{i}k}\psi_k(\varsigma), \quad \varpi_{\mathfrak{i}\mathfrak{i}} > 0,\ \mathfrak{i} = 1, 2, \ldots.$$

Where $\{\psi_{\mathfrak{i}}\}_{\mathfrak{i}=1}^{\infty}$ denotes the function system in $W_2^2[0,T]$ that can be determined in the following way

$$\begin{aligned}\psi_{\mathfrak{i}}(\varsigma) &= \mathfrak{O}^*\kappa_{\mathfrak{i}}(\varsigma)\\ &= \langle \mathfrak{O}^*\kappa_{\mathfrak{i}}(\eta), S_{\varsigma}(\eta)\rangle_{W_2^2}\\ &= \langle \kappa_{\mathfrak{i}}(\eta), \mathfrak{O}S_{\varsigma}(\eta)\rangle_{W_2^1}\\ &= \langle R_{\eta_{\mathfrak{i}}}(\eta), \mathfrak{O}S_{\varsigma}(\eta)\rangle_{W_2^1}\\ &= \mathfrak{O}_{\eta}S_{\varsigma}(\eta)|_{\eta=\varsigma_{\mathfrak{i}}},\end{aligned}$$

the operator $\mathfrak{O}_{\eta}$ is introduced to tell that $\mathfrak{O}$ is applied to η.

And, the coefficients $\varpi_{\mathfrak{i}k}$ are the orthogonalization which take the following values:

$$\varpi_{\mathfrak{i}\mathfrak{j}} = \begin{cases} \dfrac{1}{\|\psi_1\|}, & \text{for} \quad \mathfrak{i} = \mathfrak{j} = 1,\\ \dfrac{1}{e_{\mathfrak{i}}}, & \text{for} \quad \mathfrak{i} = \mathfrak{j} \neq 1,\\ -\dfrac{1}{e_{\mathfrak{i}}}\displaystyle\sum_{k=\mathfrak{j}}^{\mathfrak{i}-1} C_{\mathfrak{i}k}\varpi_{k\mathfrak{j}}, & \text{for} \quad \mathfrak{i} > \mathfrak{j}, \end{cases}$$

where $e_{\mathfrak{i}} = \sqrt{\|\psi_{\mathfrak{i}}\|^2 - \sum_{k=1}^{\mathfrak{i}-1} C_{\mathfrak{i}k}^2}, C_{\mathfrak{i}k} = \left\langle \psi_{\mathfrak{i}}, \bar{\psi}_k \right\rangle_{W_2^2}$.

Theorem 3.1. *Suppose* $\{\varsigma_{\mathfrak{i}}\}_{\mathfrak{i}=1}^{\infty}$ *is dense in* $[0,T]$, *then* $\{\psi_{\mathfrak{i}}\}_{\mathfrak{i}=1}^{\infty}$ *is the complete system of* $W_2^2[0,T]$.

Proof. We know that $\psi_{\mathfrak{i}}(\varsigma) \in W_2^2[0,T]$. So, for each fixed $g(\varsigma) \in W_2^2[0,T]$, it follows

$$\langle g(\varsigma), \psi_{\mathfrak{i}}(\varsigma)\rangle_{W_2^2} = 0,\ \mathfrak{i} = 1, 2, \ldots.$$

Since

$$\langle g(\varsigma), \psi_{\mathfrak{i}}(\varsigma)\rangle_{W_2^2} = \langle g(\varsigma), \mathfrak{O}^*\kappa_{\mathfrak{i}}(\varsigma)\rangle_{W_2^2} = \langle \mathfrak{O}g(\varsigma), \kappa_{\mathfrak{i}}(\varsigma)\rangle_{W_2^1} = \mathfrak{O}g(\varsigma_{\mathfrak{i}}) = 0,$$

and $\{\varsigma_{\mathfrak{i}}\}_{\mathfrak{i}=1}^{\infty}$ is dense on the interval $[0,T]$, we have

$$\mathfrak{O}g(\varsigma) = 0.$$

Then,

$$\mathfrak{O}^{-1}\left(\mathfrak{O}g(\varsigma)\right) = \mathfrak{O}^{-1}\left(0\right)$$

gives

$$g(\varsigma) = 0.$$

□

Lemma 3.1. *Assume* $g(\varsigma) \in W_2^2[0,T]$, *then*

$$\left\| g^{(\mathfrak{i})}(\varsigma) \right\|_C \leq \mathfrak{C} \left\| g(\varsigma) \right\|_{W_2^2}, \quad \mathfrak{i} = 0, 1,$$

where $\mathfrak{C} \geq 0$ *and* $\left\| g(\varsigma) \right\|_C = \max_{\varsigma \in [0,T]} |g(\varsigma)|$.

Proof. $\forall \varsigma \in [0,T]$ we have

$$g^{(\mathfrak{i})}(\varsigma) = \left\langle g(.), \partial_\varsigma^{(\mathfrak{i})} S_\varsigma(.) \right\rangle_{W_2^2}, \quad \mathfrak{i} = 0, 1.$$

Using the expression of $\partial_\varsigma^{(\mathfrak{i})} S_\varsigma(.)$, we can reach

$$\left\| \partial_\varsigma^{(\mathfrak{i})} S_\varsigma \right\|_{W_2^2} \leq \mathfrak{C}_\mathfrak{i}, \quad \mathfrak{i} = 0, 1.$$

Consequently,

$$\left| g^{(\mathfrak{i})}(\varsigma) \right| = \left| \left\langle g(.), \partial_\varsigma^{(\mathfrak{i})} S_\varsigma(.) \right\rangle_{W_2^2} \right| \leq \left\| \partial_\varsigma^{(\mathfrak{i})} S_\varsigma \right\|_{W_2^2} \left\| g \right\|_{W_2^2} \leq \mathfrak{C}_\mathfrak{i} \left\| g \right\|_{W_2^2}, \ \mathfrak{i} = 0, 1. \quad (3.5)$$

Where $\mathfrak{C} = \max_{\mathfrak{i}=0,1} \{\mathfrak{C}_\mathfrak{i}\}$. Then Lemma 3.1 follows from (3.5). □

Theorem 3.2. *Assume* $\{\varsigma_\mathfrak{i}\}_{\mathfrak{i}=1}^{\infty}$ *is dense in* $[0,T]$ *and problem* (3.4) *has a solution that should be unique on* $W_2^2[0,T]$. *Therefore, the solution of* (3.4) *is*

$$g(\varsigma) = \sum_{\mathfrak{i}=1}^{\infty} \sum_{k=1}^{\mathfrak{i}} \varpi_{\mathfrak{i}k} \Lambda(\varsigma_k, g(\varsigma_k)) \bar{\psi}_\mathfrak{i}(\varsigma). \quad (3.6)$$

While the solution of (3.1) *is*

$$f(\varsigma) = \sum_{\mathfrak{i}=1}^{\infty} \sum_{k=1}^{\mathfrak{i}} \varpi_{\mathfrak{i}k} \Lambda(\varsigma_k, g(\varsigma_k)) \bar{\psi}_\mathfrak{i}(\varsigma) + \lambda.$$

Proof. Firstly, the fact that $\left\{\bar{\psi}_\mathfrak{i}(\varsigma)\right\}_{\mathfrak{i}=1}^{\infty}$ is a complete orthonormal basis in $W_2^2[0,T]$ allows us to write

$$\begin{aligned}
g(\varsigma) &= \sum_{\mathfrak{i}=1}^{\infty} \left\langle g(\varsigma), \bar{\psi}_\mathfrak{i}(\varsigma) \right\rangle_{W_2^2} \bar{\psi}_\mathfrak{i}(\varsigma) \\
&= \sum_{\mathfrak{i}=1}^{\infty} \left\langle g(\varsigma), \sum_{k=1}^{\mathfrak{i}} \varpi_{\mathfrak{i}k} \psi_k(\varsigma) \right\rangle_{W_2^2} \bar{\psi}_\mathfrak{i}(\varsigma) \\
&= \sum_{\mathfrak{i}=1}^{\infty} \sum_{k=1}^{\mathfrak{i}} \varpi_{\mathfrak{i}k} \left\langle g(\varsigma), \psi_k(\varsigma) \right\rangle_{W_2^2} \bar{\psi}_\mathfrak{i}(\varsigma) \\
&= \sum_{\mathfrak{i}=1}^{\infty} \sum_{k=1}^{\mathfrak{i}} \varpi_{\mathfrak{i}k} \left\langle g(\varsigma), \mathfrak{O}^* \kappa_k(\varsigma) \right\rangle_{W_2^2} \bar{\psi}_\mathfrak{i}(\varsigma) \\
&= \sum_{\mathfrak{i}=1}^{\infty} \sum_{k=1}^{\mathfrak{i}} \varpi_{\mathfrak{i}k} \left\langle \mathfrak{O} g(\varsigma), \kappa_k(\varsigma) \right\rangle_{W_2^1} \bar{\psi}_\mathfrak{i}(\varsigma)
\end{aligned}$$

$$= \sum_{\mathfrak{i}=1}^{\infty} \sum_{k=1}^{\mathfrak{i}} \varpi_{\mathfrak{i}k} \left\langle \mathfrak{O} g(\varsigma), R_{\varsigma}(\varsigma_k) \right\rangle_{W_2^1} \bar{\psi}_{\mathfrak{i}}(\varsigma)$$
$$= \sum_{\mathfrak{i}=1}^{\infty} \sum_{k=1}^{\mathfrak{i}} \varpi_{\mathfrak{i}k} \Lambda(\varsigma_k, g(\varsigma_k)) \bar{\psi}_{\mathfrak{i}}(\varsigma),$$

with $\Lambda(\varsigma_k, g(\varsigma_k)) = \mathfrak{O} g(\varsigma_k)$.

Secondly, by substituting $g(\varsigma)$ with its value (3.6) in the transformation (3.2), we get

$$f(\varsigma) = \sum_{\mathfrak{i}=1}^{\infty} \sum_{k=1}^{\mathfrak{i}} \varpi_{\mathfrak{i}k} \Lambda(\varsigma_k, g(\varsigma_k)) \bar{\psi}_{\mathfrak{i}}(\varsigma) + \lambda.$$

□

We now write the RKHSM's solution $g_n(\varsigma)$ as

$$g_n(\varsigma) = \sum_{\mathfrak{i}=1}^{n} \sum_{k=1}^{\mathfrak{i}} \varpi_{\mathfrak{i}k} \Lambda(\varsigma_k, g(\varsigma_k)) \bar{\psi}_{\mathfrak{i}}(\varsigma).$$

The space $W_2^2[0,T]$ is a Hilbert space, so this latter implies that

$$\sum_{\mathfrak{i}=1}^{\infty} \sum_{k=1}^{\mathfrak{i}} \varpi_{\mathfrak{i}k} \Lambda(\varsigma_k, g(\varsigma_k)) \bar{\psi}_{\mathfrak{i}}(\varsigma) < \infty,$$

we conclude, then, that $g_n(\varsigma)$ converges to $g(\varsigma)$ in the norm.

Theorem 3.3. *1. The approximate solution $g_n(\varsigma)$ converges uniformly to $g(\varsigma)$.*

2. The approximate solution $g_n'(\varsigma)$ converges uniformly to $g'(\varsigma)$.

Proof. For the first result, we need to estimate the term on the left below: $\forall \varsigma \in [0,T]$,

$$\begin{aligned} |g_n(\varsigma) - g(\varsigma)| &= \left| \langle g_n(\centerdot) - g(\centerdot), S_{\varsigma}(\centerdot) \rangle_{W_2^2} \right| \\ &\leq \|S_{\varsigma}\|_{W_2^2} \|g_n - g\|_{W_2^2} \\ &\leq \mathcal{C}_0 \|g_n - g\|_{W_2^2}, \end{aligned}$$

where $\mathcal{C}_0$ is a constant.

Following the same way, we get

$$|g_n'(\varsigma) - g'(\varsigma)| \leq \|\partial_{\varsigma} S_{\varsigma}\|_{W_2^2} \|g_n' - g'\|_{W_2^2},$$

due to the uniform boundedness of $\partial_{\varsigma} S_{\varsigma}(\centerdot)$, we have

$$\|\partial_{\varsigma} S_{\varsigma}\|_{W_2^2} \leq \mathcal{C}_1,$$

where $\mathcal{C}_1$ is a positive constant.

Therefore

$$|g_n'(\varsigma) - g'(\varsigma)| \leq \mathcal{C}_1 \|g_n' - g'\|_{W_2^2}.$$

□

4. A numerical experiment

This section is the numerical part that assures the efficiency of the new method. The logistic differential equation is discussed in Example 4.1, the Riccati differential equation is considered in Example 4.2, and a NODE is discussed in Example 4.3.

Example 4.1. Taking the non-linear logistic differential equation:

$$\begin{cases} f'(\varsigma) = \dfrac{1}{2} f(\varsigma)\left(1 - f(\varsigma)\right), \quad \varsigma \in [0, 10], \\ f(0) = \dfrac{1}{2}, \end{cases} \tag{4.1}$$

that has the following exact solution:

$$f(\varsigma) = \frac{e^{\frac{\varsigma}{2}}}{1 + e^{\frac{\varsigma}{2}}}.$$

We start with homogenizing the initial condition $f(0) = \frac{1}{2}$ and this involves defining the new function: $g(\varsigma) = f(\varsigma) - \frac{1}{2}$.

Using it, the new problem will be

$$\begin{cases} g'(\varsigma) = \dfrac{1}{2}\left(\dfrac{1}{4} - g^2(\varsigma)\right), \quad \varsigma \in [0, 10], \\ g(0) = 0. \end{cases} \tag{4.2}$$

Now, by taking the Laplace transform of the left- and right-hand sides of (4.2), it becomes

$$s\mathcal{L}\left[g(\varsigma)\right] = \frac{1}{2}\left(\frac{1}{4s} - \mathcal{L}\left[g^2(\varsigma)\right]\right).$$

Then, we obtain

$$\mathcal{L}\left[g(\varsigma)\right] = \frac{1}{2s}\left(\frac{1}{4s} - \mathcal{L}\left[g^2(\varsigma)\right]\right),$$

which has the following inverse transform

$$g(\varsigma) = \mathcal{L}^{-1}\left[\frac{1}{2s}\left(\frac{1}{4s} - \mathcal{L}\left[g^2(\varsigma)\right]\right)\right].$$

To carry on, it is necessary to introduce a bounded linear operator $\mathfrak{O}$ as

$$\begin{aligned} &\mathfrak{O}: \ W_2^2[0, 10] \ \longrightarrow \ W_2^1[0, 10], \\ &g(\varsigma) \ \longrightarrow \ \mathfrak{O}\left(g(\varsigma)\right) = g(\varsigma). \end{aligned}$$

Thus, we reach the step of the application of the RKHSM as we said before. Taking $n = 25$ collocation points in which $\varsigma = \frac{\mathfrak{i}}{n}$, $\mathfrak{i} = 1, 2 \ldots, n$. The approximate solution for Example 4.1 is found using the new L-RKHSM and it is compared with its exact and RKHSM's solution. Table 1 shows the exact solution, the solutions that are obtained by using the new L-RKHSM, and the classical RKHSM with their absolute errors in a large domain $[0, 10]$. In this table, we obtained results by the L-RKHSM and they are much better than those of the classical RKHSM with a

minute number of iterations. In Figure 11 we compared the exact solution with the L-RKHSM's solution whereas in Figure 12 we compared the exact solution with the classical RKHSM's solution. Figure 3 is where the three solutions are depicted together. We can see from these figures that the graphs' behavior is very similar. To highlight more comparisons between the L-RKHSM and the RKHSM, we drew the absolute error of both methods in Figures 4 and 5. What we can observe here is that the L-RKHSM's solution is very close to the exact solution, unlike the classical RKHSM. And this confirms that the L-RKHSM is more effective compared with the RKHSM. One of the powerful advantages of this new method is we can obtain better results than the classical RKHSM with a minute number of iterations.

Table 1. Numerical results of Example 4.1.

				Absolute Error of	
ς	Exact solution	L-RKHSM	RKHSM	L-RKHSM	RKHSM
0.0	0.5000000000	0.5000000000	0.5000000000	0.00000	0.00000
1.0	0.6224593312	0.6223461978	0.6158563195	1.13133×10^{-4}	6.60301×10^{-3}
2.0	0.7310585786	0.7309895126	0.7251869079	6.90660×10^{-5}	5.87167×10^{-3}
3.0	0.8175744762	0.8174733093	0.8126519688	1.01167×10^{-4}	4.92250×10^{-3}
4.0	0.8807970780	0.8807161835	0.8768334171	8.08945×10^{-5}	3.96366×10^{-3}
5.0	0.9241418200	0.9241052546	0.9210617450	3.65654×10^{-5}	3.08008×10^{-3}
6.0	0.9525741268	0.9525763640	0.9502585348	2.23720×10^{-6}	2.31559×10^{-3}
7.0	0.9706877692	0.9707129324	0.9689970890	2.51632×10^{-5}	1.69068×10^{-3}
8.0	0.9820137900	0.9820472917	0.9808099544	3.35017×10^{-5}	1.20384×10^{-3}
9.0	0.9890130574	0.9890454610	0.9881728305	3.24036×10^{-5}	8.40227×10^{-4}
10	0.9933071491	0.9933356208	0.9927303315	2.84717×10^{-5}	5.76818×10^{-4}

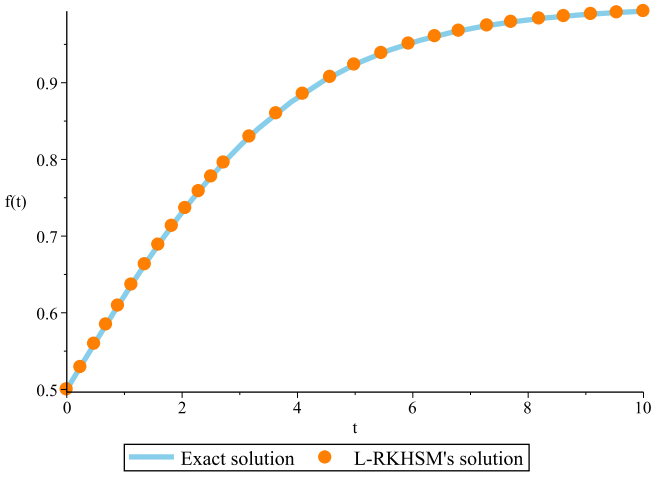

Figure 1. Exact and L-RKHSM's solutions for Example 4.1.

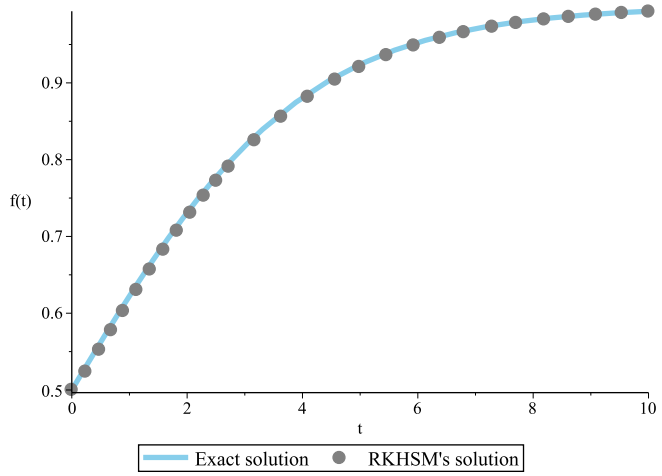

Figure 2. Exact and RKHSM's solutions for Example 4.1.

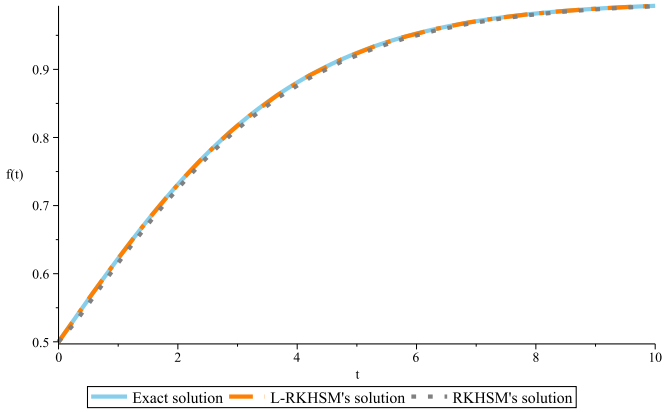

Figure 3. Comparison between the three solutions: the Exact, L-RKHSM, and RKHSM solutions for Example 4.1.

Example 4.2. Taking the Riccati differential equation:

$$\begin{cases} f'(\varsigma) = t^3 f^2(\varsigma) - 2\varsigma^4 f(\varsigma) + \varsigma^5 + 1, \quad \varsigma \in [0,1], \\ f(0) = 0, \end{cases} \tag{4.3}$$

that has the following exact solution:

$$f(\varsigma) = \varsigma.$$

We start with taking the Laplace transform of the left- and right-hand sides of (4.3) directly because the initial condition of this problem is already homogeneous.

So, the equation (4.3) becomes

$$s\mathcal{L}\left[f(\varsigma)\right] = \mathcal{L}\left[\varsigma^3 f^2(\varsigma)\right] - \mathcal{L}\left[2\varsigma^4 f(\varsigma)\right] + \frac{120}{s^6} + \frac{1}{s}.$$

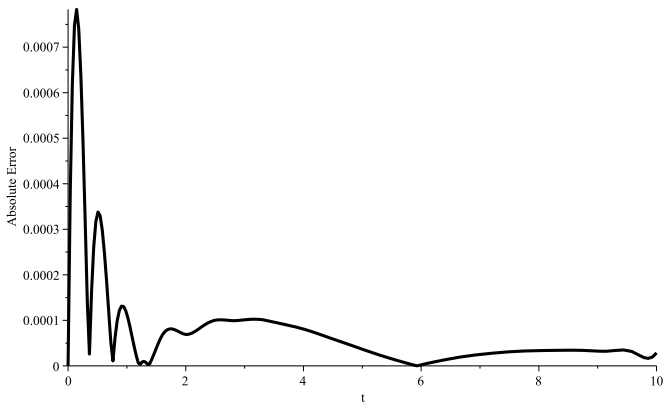

Figure 4. Absolute error of the L-RKHSM for Example 4.1.

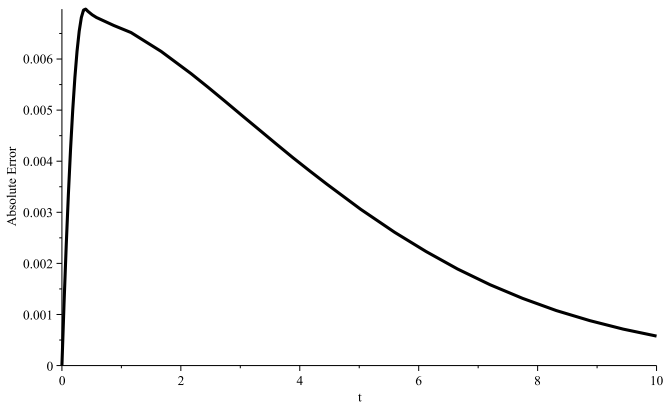

Figure 5. Absolute error of the RKHSM for Example 4.1.

Then, we obtain

$$\mathcal{L}\left[f(\varsigma)\right] = \frac{1}{s}\left(\mathcal{L}\left[\varsigma^3 f^2(\varsigma)\right] - \mathcal{L}\left[2\varsigma^4 f(\varsigma)\right] + \frac{120}{s^6} + \frac{1}{s}\right),$$

which has the following inverse transform

$$f(\varsigma) = \mathcal{L}^{-1}\left[\frac{1}{s}\left(\mathcal{L}\left[\varsigma^3 f^2(\varsigma)\right] - \mathcal{L}\left[2\varsigma^4 f(\varsigma)\right] + \frac{120}{s^6} + \frac{1}{s}\right)\right].$$

To carry on, it is necessary to introduce a bounded linear operator $\mathfrak{O}$ as

$$\begin{aligned} &\mathfrak{O} : W_2^2[0,1] \;\longrightarrow\; W_2^1[0,1], \\ &f(\varsigma) \;\longrightarrow \mathfrak{O}\left(f(\varsigma)\right) = f(\varsigma). \end{aligned}$$

Thus, we reach the step of the application of the RKHSM as we said before. Taking $n = 25$ collocation points in which $\varsigma = \frac{\mathfrak{i}}{n}$, $\mathfrak{i} = 1, 2 \ldots, n$. The approximate solution for Example 4.2 is found using the new L-RKHSM and it is compared with

its exact and RKHSM's solution. Table 2 shows the exact solution, the solutions that are obtained by using the new L-RKHSM, and the classical RKHSM with their absolute errors when $\varsigma \in [0,1]$. In this table, we obtained results by the L-RKHSM and they are much better than those of the classical RKHSM with a minute number of iterations. In Figure 6 we compared the exact solution with the L-RKHSM's solution whereas in Figure 7 we compared the exact solution with the classical RKHSM's solution. Figure 8 is where the three solutions are depicted together. We can see from these figures that the graphs' behavior is very similar. To highlight more comparisons between the L-RKHSM and the RKHSM, we drew the absolute error of both methods in Figures 9 and 10. What we can observe here is that the L-RKHSM's solution is very close to the exact solution, unlike the classical RKHSM. And this confirms that the L-RKHSM is more effective compared with the RKHSM.

Table 2. Numerical results of Example 4.2.

				Absolute Error of	
ς	Exact solution	L-RKHSM	RKHSM	L-RKHSM	RKHSM
0.0	0.0	0.0	0.0	0.0	0.0
0.1	0.1	0.0999948043	0.0992307635	5.2×10^{-6}	7.69237×10^{-4}
0.2	0.2	0.2000000002	0.1992307639	2.0×10^{-10}	7.69236×10^{-4}
0.3	0.3	0.3000000067	0.2992307647	6.7×10^{-9}	7.69235×10^{-4}
0.4	0.4	0.3999999998	0.3992307675	2.0×10^{-10}	7.69233×10^{-4}
0.5	0.5	0.4999999972	0.4992307730	2.8×10^{-9}	7.69227×10^{-4}
0.6	0.6	0.6000000009	0.5992307823	9.0×10^{-10}	7.69218×10^{-4}
0.7	0.7	0.7000000008	0.6992307992	8.0×10^{-10}	7.69201×10^{-4}
0.8	0.8	0.7999999868	0.7992308244	1.3×10^{-8}	7.69176×10^{-4}
0.9	0.9	0.8999999893	0.8992308608	1.1×10^{-8}	7.69139×10^{-4}
1.0	1.0	0.9999999839	0.9992309114	1.6×10^{-8}	7.69089×10^{-4}

Example 4.3. Taking the non-linear ODE:

$$\begin{cases} f'(\varsigma) - 1 = f^2(\varsigma), \quad \varsigma \in [0,1], \\ f(0) = 0, \end{cases} \tag{4.4}$$

that has the following exact solution :

$$f(\varsigma) = \tan(\varsigma).$$

We start with taking the Laplace transform of the left- and right-hand sides of (4.4) directly because the initial condition of this problem is already homogeneous.

So, the equation (4.4) becomes

$$s\mathcal{L}\left[f(\varsigma)\right] = \mathcal{L}\left[f^2(\varsigma)\right] + \frac{1}{s}.$$

Then, we obtain

$$\mathcal{L}\left[f(\varsigma)\right] = \frac{1}{s}\left(\mathcal{L}\left[f^2(\varsigma)\right] + \frac{1}{s}\right),$$

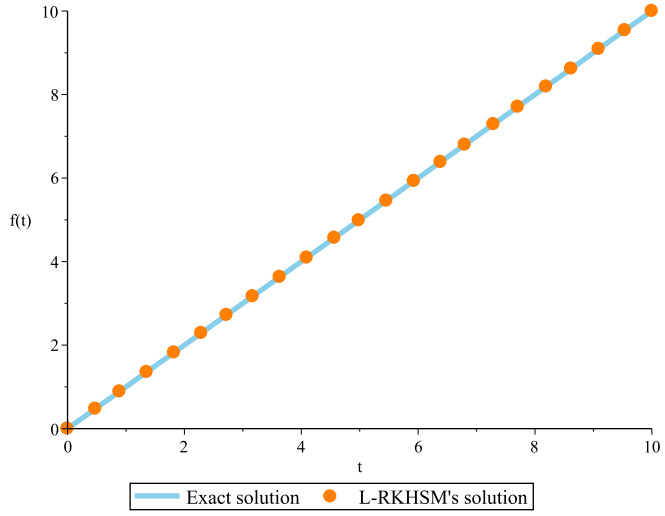

Figure 6. Exact and L-RKHSM's solutions for Example 4.2.

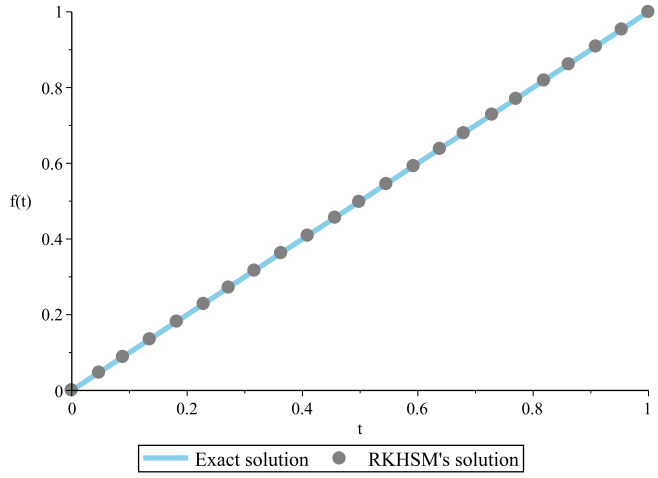

Figure 7. Exact and RKHSM's solutions for Example 4.2.

which has the following inverse transform

$$f(\varsigma) = \mathcal{L}^{-1}\left[\frac{1}{s}\left(\mathcal{L}\left[f^2(\varsigma)\right] + \frac{1}{s}\right)\right].$$

To carry on, it is necessary to introduce a bounded linear operator $\mathfrak{O}$ as

$$\mathfrak{O} : W_2^2[0,1] \longrightarrow W_2^1[0,1],$$
$$f(\varsigma) \longrightarrow \mathfrak{O}\left(f(\varsigma)\right) = f(\varsigma).$$

Thus, we reach the step of the application of the RKHSM as we said before. Taking $n = 25$ collocation points in which $\varsigma = \frac{\mathfrak{i}}{n}$, $\mathfrak{i} = 1, 2 \ldots, n$. The approximate

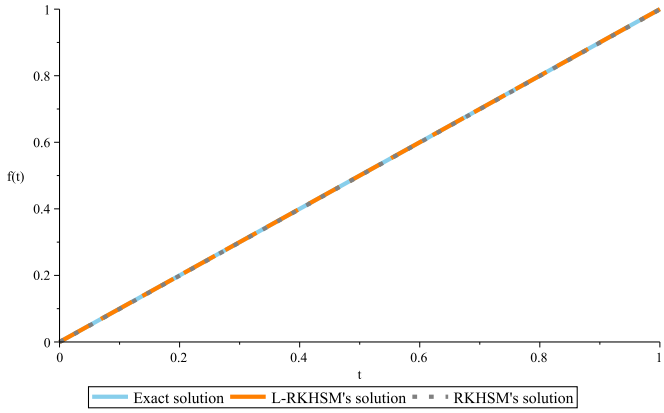

Figure 8. Comparison between the three solutions: the Exact, L-RKHSM, and RKHSM solutions for Example 4.2.

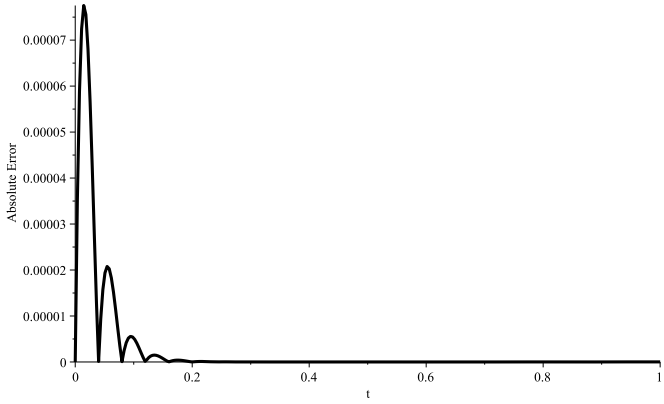

Figure 9. Absolute error of the L-RKHSM for Example 4.2.

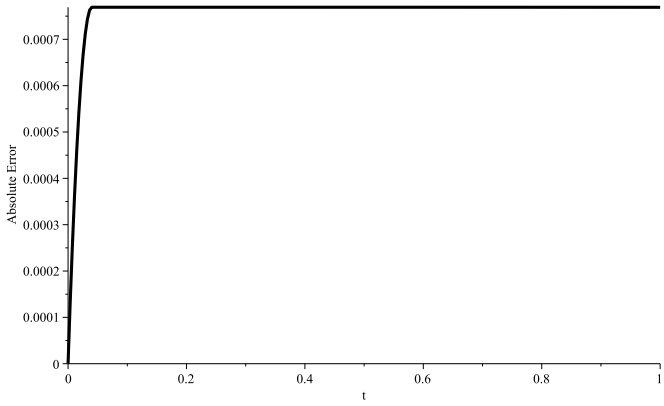

Figure 10. Absolute error of the RKHSM for Example 4.2.

solution for Example 4.3 is found using the new L-RKHSM and it is compared with

its exact and RKHSM's solution. Table 3 shows the exact solution, the solutions that are obtained by using the new L-RKHSM, and the classical RKHSM with their absolute errors when $\varsigma \in [0, 1]$. In this table, we obtained results by the L-RKHSM and they are much better than those of the classical RKHSM with a minute number of iterations. In Figure 11 we compared the exact solution with the L-RKHSM's solution whereas in Figure 12 we compared the exact solution with the classical RKHSM's solution. Figure 13 is where the three solutions are depicted together. We can see from these figures that the graphs' behavior is very similar. To highlight more comparisons between the L-RKHSM and the RKHSM, we drew the absolute error of both methods in Figures 14 and 15. What we can observe here is that the L-RKHSM's solution is very close to the exact solution, unlike the classical RKHSM. And this confirms that the L-RKHSM is more effective compared with the RKHSM.

Table 3. Numerical results of Example 4.3.

				Absolute Error of	
ς	Exact solution	L-RKHSM	RKHSM	L-RKHSM	RKHSM
0.0	0.0	0.0	0.0	0.0	0.0
0.1	0.1003346721	0.1003315842	0.0995220122	3.08790×10^{-6}	8.12660×10^{-4}
0.2	0.2027100355	0.2027072115	0.2018952901	2.82400×10^{-6}	8.14745×10^{-4}
0.3	0.3093362496	0.3093290983	0.3084928946	7.15130×10^{-6}	8.43355×10^{-4}
0.4	0.4227932187	0.4227787500	0.4218831247	1.44687×10^{-5}	9.10094×10^{-4}
0.5	0.5463024898	0.5462744286	0.5452686924	2.80612×10^{-5}	1.03380×10^{-3}
0.6	0.6841368083	0.6840852256	0.6828861202	5.15827×10^{-5}	1.25069×10^{-3}
0.7	0.8422883805	0.8421937224	0.8406636025	9.46581×10^{-5}	1.62478×10^{-3}
0.8	1.0296385570	1.0294591450	1.0273488640	1.79412×10^{-4}	2.28970×10^{-3}
0.9	1.2601582180	1.2598541310	1.2566416090	3.04087×10^{-4}	3.51661×10^{-3}
1.0	1.5574077250	1.5566408810	1.5514464480	7.66844×10^{-4}	5.96128×10^{-3}

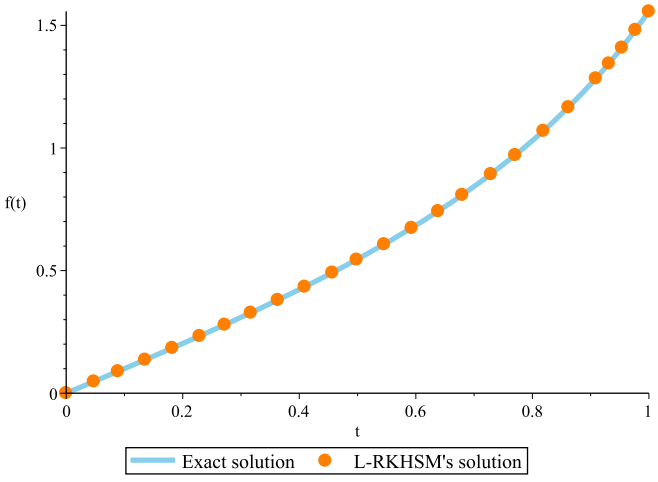

Figure 11. Exact and L-RKHSM's solutions for Example 4.3.

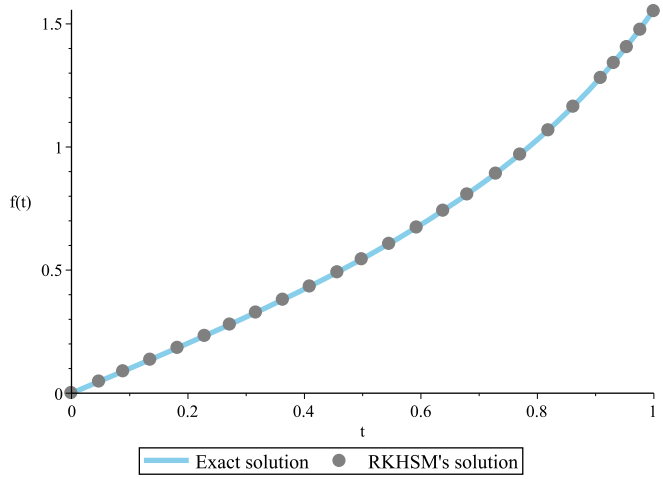

Figure 12. Exact and RKHSM's solutions for Example 4.3.

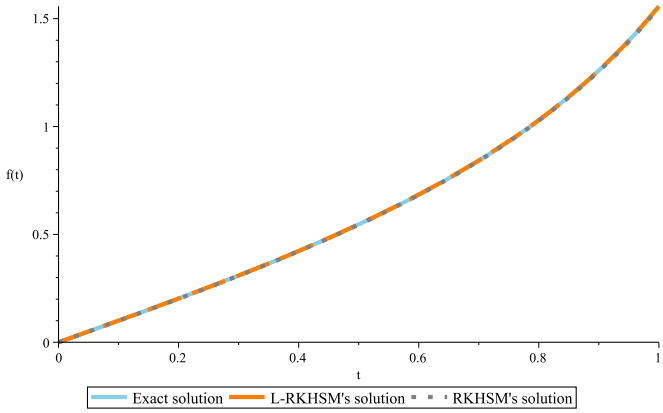

Figure 13. Comparison between the three solutions: the Exact, L-RKHSM, and RKHSM solutions for Example 4.3.

5. Conclusion

In this paper, we successfully introduced an efficient novel method, named the Laplace-Reproducing Kernel Hilbert Space Method, for solving non-linear ordinary differential equations. By combining the reproducing kernel Hilbert space method with the Laplace transformation, the L-RKHSM achieves enhanced accuracy and applicability. The method was validated through three distinct applications, demonstrating its effectiveness in producing accurate numerical solutions with a minimal number of iterations compared to the classical RKHSM. The results show that the L-RKHSM is a powerful and versatile tool for addressing a wide variety of non-linear problems that arise in various physical contexts. This new approach not only offers significant improvements in computational efficiency but also expands the potential for solving complex non-linear ODEs, making it a valuable addition to the toolbox of numerical methods in engineering and physics. Future work could explore

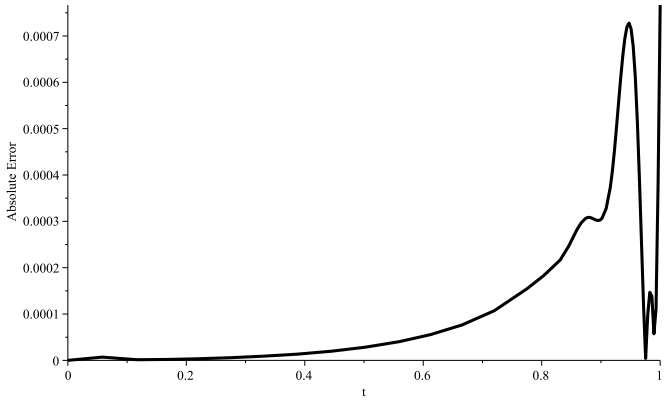

Figure 14. Absolute error of the L-RKHSM for Example 4.3.

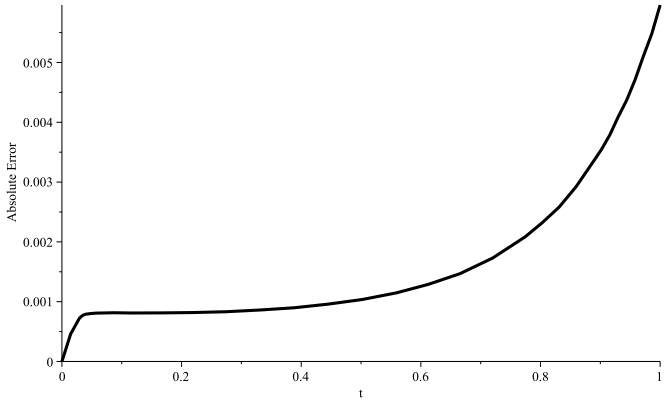

Figure 15. Absolute error of the RKHSM for Example 4.3.

further applications of the L-RKHSM to other types of differential equations and investigate potential enhancements to the method.

Acknowledgements

The authors thank the reviewers for their helpful comments and suggestions, which improved the paper.

References

[1] O. Abu Arqub, J. Singh, B. Maayah and M. Alhodaly, *Reproducing kernel approach for numerical solutions of fuzzy fractional initial value problems under the Mittag-Leffler kernel differential operator*, Math. Meth. Appl. Sci., 2023, 46(7), 7965–7986.

[2] A. Akgül, *A novel method for a fractional derivative with non-local and non-singular kernel*, Chaos Solit. Fractals, 2018, 114, 478–482.

[3] A. Akgül, A. Cordero and J. R. Torregrosa, *Solutions of fractional gas dynamics equation by a new technique*, Math. Meth. Appl. Sci., 2020, 43, 1349–1358.

[4] T. Allahviranloo and H. Sahihi, *Reproducing kernel method to solve fractional delay differential equations*, App. Math. Comput., 2021, 400, 126095.

[5] F. M. Allehiany, M. H. DarAssi, I. Ahmad, M. A. Khan and E. M. Tag-Eldin, *Mathematical Modeling and backward bifurcation in monkeypox disease under real observed data*, Results Phys., 2023, 20, 106557.

[6] A. M. Alqahtani, M. Ould Sidi, M. R. Khan, M. A. Elkotb, E. Tag-Eldin and A. M. Galal, *Transport properties of two-dimensional dissipative flow of hybrid nanofluid with Joule heating and thermal radiation*, Sci. Rep., 2022, 12(1), 19374.

[7] A. Atangana and A. Akgül, *On solutions of fractal fractional differential equations*, Discrete Contin. Dyn. Syst. Ser. A, 2021, 14(10), 3441–3457.

[8] N. Attia, A. Akgül, D. Seba and A. Nour, *An efficient numerical technique for a biological population model of fractional order*, Chaos Solit. Fractals, 2020, 141, 110349.

[9] A. Attia, A. Akgül, D. Seba and A. Nour, *On solutions of time-fractional advection-diffusion equation*, Numer. Methods Partial Differ. Equ., 2023, 39(6), 4489–4516.

[10] B. Azarnavid, *The Bernoulli polynomials reproducing kernel method for nonlinear Volterra integro-differential equations of fractional order with convergence analysis*, Comput. Appl. Math., 2022, 42(1), 8.

[11] E. Babolian, S. Javadi and E. Moradi, *RKM for solving Bratu-type differential equations of fractional order*, Math. Meth. Appl. Sci., 2016, 39(6), 1548–1557.

[12] H. Beyrami and T. Lotfi, *A novel method with error analysis for the numerical solution of a logarithmic singular Fredholm integral equation*, Afr. Mat., 2023, 34(2), 33.

[13] Y. Chellouf, B. Maayah, S. Momani, A. Alawneh and S. Alnabulsi, *Numerical solution of fractional differential equations with temporal two-point BVPs using reproducing kernal Hilbert space method*, AIMS Math., 2021, 6(4), 3465–3485.

[14] M. Cui and Y. Lin, *Nonlinear Numerical Analysis in the Reproducing Kernel Space*, Nova Science Publishers, Inc, New York, 2009.

[15] F. Z. Geng, *Numerical methods for solving Schrödinger equations in complex reproducing kernel Hilbert spaces*, Math. Sci., 2020, 14(4), 293–299.

[16] F. Geng and M. Cui, *New method based on the HPM and RKHSM for solving forced Duffing equations with integral boundary conditions*, J. Comput. Appl. Math., 2009, 233(2), 165–172.

[17] F. Geng and M. Cui, *A reproducing kernel method for solving nonlocal fractional boundary value problems*, Appl. Math. Lett., 2012, 25(5), 818–823.

[18] B. Ghanbari and A. Akgül, *Abundant new analytical and approximate solutions to the generalized Schamel equation*, Phys. Scr., 2020, 95(7), 075201.

[19] A. Ghasemi and A. Saadatmandi, *A new Bernstein-reproducing kernel method for solving forced Duffing equations with integral boundary conditions*, CMDE, 2024, 12(2), 329–337.

[20] N. Harrouche, S. Momani, S. Hasan and M. Al-Smadi, *Computational algorithm for solving drug pharmacokinetic model under uncertainty with nonsingular kernel type Caputo-Fabrizio fractional derivative*, Alex. Eng. J., 2021, 60(5), 4347–4362.

[21] F. Hemati, M. Ghasemi and G. R. Khoshsiar, *Numerical solution of the multiterm time-fractional diffusion equation based on reproducing kernel theory*, Numer. Methods Partial Differ. Equ., 2021, 37(1), 44–68.

[22] S. M. E. Ismaeel, Abdul-Majid Wazwaz, E. Tag-Eldin and S. A. El-Tantawy, *Simulation studies on the dissipative modified Kawahara solitons in a complex plasma*, Symmetry, 2023, 15(1), 57.

[23] W. Jiang and T. Tian, *Numerical solution of nonlinear Volterra integro-differential equations of fractional order by the reproducing kernel method*, Appl. Math. Model., 2015, 39(16), 4871–4876.

[24] M. Modanli and A. Akgül, *On solutions to the second-order partial differential equations by two accurate methods*, Numer. Methods Partial Differ. Equ., 2018, 34(5), 1678–1692.

[25] S. Momani, N. Djeddi, M. Al-Smadi and S. Al-Omari, *Numerical investigation for Caputo-Fabrizio fractional Riccati and Bernoulli equations using iterative reproducing kernel method*, Appl. Numer. Math., 2021, 170, 418–434.

[26] M. G. Sakar, *Iterative reproducing kernel Hilbert spaces method for Riccati differential equation*, J. Comput. Appl. Math., 2017, 309, 163–174.

[27] M. G. Sakar, O. Saldır and A. Akgül, *A novel technique for fractional Bagley-Torvik equation*, Proc. Natl. Acad. Sci., India, Sect. A Phys. Sci., 2019, 89, 539–545.

[28] S. A. A. Shah, N. A. Ahammad, B. Ali, K. Guedri, Aziz Ullah Awan, F. Gamaoun and E. M. Tag-ElDin, *Significance of bio-convection, MHD, thermal radiation and activation energy across Prandtl nanofluid flow: A case of stretching cylinder*, Int. Commun. Heat Mass Transf., 2022, 137, 106299.

[29] L. Shi, S. Tayebi, O. Abu Arqub, M. S. Osman, P. Agarwal, W. Mahamoud, M. Abdel-Aty and M. Alhodaly, *The novel cubic B-spline method for fractional Painlevé and Bagley-Trovik equations in the Caputo, Caputo-Fabrizio, and conformable fractional sense*, Alex. Eng. J., 2023, 65, 413–426.

[30] A. Tassaddiq, S. Qureshi, A. Soomro, O. Abu Arqub and M. Senol, *Comparative analysis of classical and Caputo models for COVID-19 spread: Vaccination and stability assessment*, Fixed Point Theory Algorithms Sci. Eng., 2024, 2024(2).

[31] S. Zaremba, *Sur le calcul numérique des fonctions demandées dans le problème de Dirichlet et le problème hydrodynamique*, Bulletin International de l'Académie des Sciences de Cracovie, 1908, 68, 125–195.